A Continuously Stratified Thermocline Model Incorporating a Mixed Layer of Variable Thickness and Density

JOHN C. MARSHALL and A. J. GEORGE NURSER

Space and Atmospheric Physics Group, Department of Physics, Imperial College, London, United Kingdom

(Manuscript received 14 September 1990, in final form 15 March 1991)

ABSTRACT

A continuously stratified, steady thermocline model is formulated in which a mixed layer of variable depth and density overlies a stratified thermocline. Rather than prescribe the distribution of density and vertical velocity at the top of the permanent thermocline, we explicitly represent the dynamics of the vertically homogeneous layer that overlies it; the density distribution at the sea surface, the depth of the mixed layer, and the structure of the thermocline are all found for prescribed patterns of Ekman pumping and surface buoyancy fluxes. If the potential vorticity of the thermocline is assumed to have a uniform value on isopycnal surfaces, it is shown that the problem can be reduced to one of finding the distribution of a single scalar field, the mixed-layer density, by the method of characteristics. Given this field and knowledge of the potential vorticity distribution in the thermocline, all other variables of the model can be found. The resulting model seems ideally suited to the study of the interaction of a mixed layer with a stratified thermocline, since it explicitly represents the lateral geostrophic flow through the sloping base of the mixed layer.

Idealized solutions are presented for both subtropical and subpolar gyres in which, in response to patterns of wind and diabatic forcing, isopycnals outcrop into a mixed layer of variable thickness and density. The effect of both warming and cooling of the mixed layer on the structure of the gyre is investigated.

1. Introduction

Here we describe the formulation of, and present solutions from, a steady thermocline model in which a continuously stratified thermocline is overlain by a vertically homogeneous mixed layer of variable depth and density, exposed to mechanical and thermodynamic forcing. The physical motivation behind such a model is set out in Woods (1985). There, emphasis is placed on the need to take account of regional variations in the depth of the mixed layer and the need to develop models that are driven by surface fluxes rather than prescribing the density of the sea surface. In the present model, an Ekman pumping field at the sea surface drives a lateral circulation in the mixed layer that flows geostrophically through its sloping base into the main thermocline. The mixed-layer density and depth are found rather than prescribed. Although the model is steady, its formulation renders it a useful tool to study the interaction between the mixed layer and the stratified thermocline if the mixed-layer depth of the model is interpreted as representing annual maximum values.

The study complements the ventilated thermocline models of Luyten et al. (1983), Huang (1988a,b; 1989), and Williams (1989). In these models the mixed-layer density and depth fields are prescribed, and the potential vorticity field in the thermocline, consistent with a given pattern of wind forcing, is then determined. The surface heat flux is diagnosed.

Instead, in the formulation of the thermocline problem developed here, it is assumed a priori that the interior potential vorticity distribution is known even on those isopycnal surfaces that outcrop into the mixed layer. This great simplification of the physics permits an elegant mathematical formulation of the thermocline problem, allowing the mixed-layer depth and temperature to vary both with latitude and longitude. We proceed to calculate the mixed-layer density and depth variation (and, through knowledge of the potential vorticity field, the structure of the thermocline) induced by prescribed wind and thermodynamic forcing. *Given only the potential vorticity distribution of the moving fluid in the thermocline, the wind stress, and the applied surface density flux, a complete solution can be found in which isopycnals outcrop into a mixed layer of variable thickness and density.*

The resulting model is clearly relevant to the entrainment regime of the subpolar gyre. We believe, however, it may also have diagnostic value in the subtropical gyre.

For simplicity, the potential vorticity distribution has been chosen to have an unchanging uniform value on each isopycnal wherever the fluid is in motion. It

Corresponding author address: Dr. J. C. Marshall, Department of Earth, Atmospheric and Planetary Sciences, Massachusetts Institute of Technology, Cambridge, MA 02139.

is not completely unrealistic; observations suggest that the gyre at depth is confined to regions where potential vorticity gradients are small, and there may be ventilated surfaces on which gradients of subducted potential vorticity may also be small (Williams 1991). However, uniform potential vorticity is best thought of as a convenient device enabling us to readily obtain physically interesting solutions *without* imposing the density and thickness of the mixed layer. Solutions are presented for idealized patterns of surface forcing for both subpolar and subtropical gyres. The influence of variations in the temperature and thickness of the mixed layer on the thermocline below is studied.

The model has also been used to study the entrainment and subduction of fluid between the mixed layer and the thermocline. The sense of the mass flux, that is, whether it is directed into or out of the mixed layer, depends on the sign of the diabatic forcing. The magnitude of the mass flux is set by the diabatic heating rate, the depth of the mixed layer, and the isopycnal spacing (the potential vorticity) at the base of the mixed layer. Study of this point using the model deserves attention in its own right and is described in detail in the companion paper, Nurser and Marshall (1991, hereafter NM).

The formulation of the model is described in section 2. In section 3 the method of solution is outlined and, in section 4, solutions for subpolar and subtropical gyres are presented.

2. Formulation of the model

We consider a steady ocean made up of a vertically homogeneous mixed layer, within which horizontal advection of heat balances prescribed diabatic sources and sinks, overlying an "ideal"—that is, inviscid and adiabatic—thermocline. The vertical structure of the model is illustrated in Fig. 1; it is in accord with the conceptual model advocated in Fig. 3 of Woods (1985). The mixed-layer thickness, h, should be interpreted as the depth to which water is mixed in winter.

The depth-integrated transport is determined by the wind stress curl—the Sverdrup constraint—but the vertical structure of the gyre depends both on the potential vorticity distribution in the thermocline and the temperature of the mixed layer. The formulation of the model is inspired by that of Niiler and Dubbelday (1970), who adopted a Needler (1967) similarity solution for the thermocline. Instead, here we invoke potential vorticity homogenization to choose an idealized but physically motivated thermocline solution.

Previous authors have shown that if the mixed-layer density is known, together with a hypothesis for the variation of potential vorticity in the moving thermocline with density (e.g., Pedlosky and Young 1983; Nurser 1988), or with density and streamline (Huang 1988a), then the Sverdrup constraint allows one to solve for the depth of the "bowl" within which the moving thermocline waters are confined. Once the depth of the bowl is known the full solution then follows.

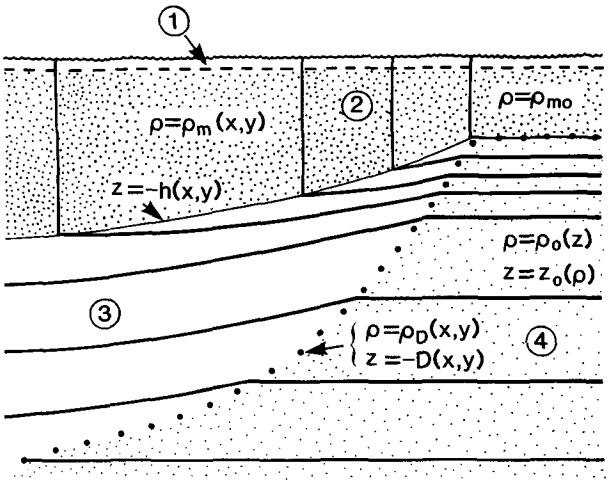

FIG. 1. A schematic diagram of the vertical structure of the model showing (1) the shallow Ekman layer (2) the vertically homogeneous mixed layer of depth $h(x, y)$ and density $\rho_m(x, y)$, (3) the moving thermocline waters separated by the "bowl" $z = -D(x, y)$ from (4) the resting abyssal fluid with reference stratification $\rho = \rho_0(z)$.

Here, rather than specifying the mixed-layer density field everywhere, we allow it to be determined from the mixed-layer thermodynamic equation. It will be shown that if the mixed-layer density is known at a given point, we can evaluate the part of the mixed-layer velocity that advects the mixed-layer density at that point. The mixed-layer thermodynamic equation can thus be expressed as a quasi-linear PDE in terms of the mixed-layer density field alone; this PDE propagates known values of the mixed-layer density on the boundary into the interior. Once the mixed-layer density field is known, the rest of the solution then follows.

The model is formulated in terms of a *local* Cartesian frame with eastward, northward, and upward coordinates x, y, and z. Results, however, are evaluated and presented in full spherical geometry.

a. The mixed layer

The mixed layer is vertically homogeneous, with density $\rho_m(x, y)$ and thickness $h(x, y)$. It is exposed to thermal and mechanical forcing. Mechanical forcing is confined to a thin surface Ekman layer; below this Ekman layer the flow is supposed to be in geostrophic and hydrostatic balance, with

$$\mathbf{u}_m = \mathbf{k} \times \nabla p_m/(\bar{\rho} f) \tag{1}$$

$$\frac{\partial p_m}{\partial z} + g\rho_m = 0 \tag{2}$$

where $p_m(x, y, z)$ is the mixed-layer pressure field, f the Coriolis parameter, $\bar{\rho}$ a mean density, and g the acceleration due to gravity.

We assume that there is no jump in density between the base of the mixed layer and the thermocline. Therefore, the density budget of the layer, separating out advection by the Ekman flux from that by the geostrophic flow, is

$$-\frac{1}{\bar{\rho}f}\mathbf{k}\times\boldsymbol{\tau}\cdot\nabla\rho_m+\int_{-h}^{0}\mathbf{u}_m\cdot\nabla\rho_m dz=-\frac{\alpha_E\mathscr{H}_{\text{in}}}{c_W} \quad (3)$$

where α_E is the expansion coefficient, $\mathscr{H}_{\text{in}}$ is the heat input/unit surface area, c_W is the specific heat of water, and $\boldsymbol{\tau}$ is the applied wind stress. Density inputs resulting from changes in salinity associated with fluxes of freshwater have been neglected, but can readily be included.

It is considerable simplification to include the advection by the Ekman flux in a net heating. So, defining

$$\mathscr{H}_{\text{net}}=\mathscr{H}_{\text{in}}-\frac{c_W}{\alpha_E\bar{\rho}f}\mathbf{k}\times\boldsymbol{\tau}\cdot\nabla\rho_m, \quad (4)$$

(3) simplifies to

$$\int_{-h}^{0}\mathbf{u}_m\cdot\nabla\rho_m dz=-\frac{\alpha_E\mathscr{H}_{\text{net}}}{c_W}. \quad (5)$$

By geostrophy and hydrostasy the velocity shear is in thermal wind balance, so

$$\mathbf{u}_m=\mathbf{k}\times\nabla p_s/(\bar{\rho}f)-gz\mathbf{k}\times\nabla\rho_m/(\bar{\rho}f) \quad (6)$$

where the surface pressure $p_s=p|_{z=0}$. Within the mixed layer, therefore, the velocity component *along* the temperature gradient is independent of depth, and we may replace $\mathbf{u}_m\cdot\nabla\rho_m$ in the integral in (5) by its surface value. Equation (5) then takes the form, dividing through by h,

$$\frac{1}{\bar{\rho}f}\mathbf{k}\times\nabla p_s\cdot\nabla\rho_m=-\frac{\alpha_E\mathscr{H}_{\text{net}}}{hc_W}. \quad (7)$$

This thermodynamic equation (7) is the key equation of our model; given p_s and h, it can be used to find the mixed-layer density field from the $\mathscr{H}_{\text{net}}$ field. In order to solve it, we will show how our assumption of uniform potential vorticity, used in conjunction with the Sverdrup constraint, allows p_s to be expressed as a function of ρ_m alone; this allows (7) to be written in a quasi-linear form and solved by the method of characteristics. We must first relate p_s to the hydrography of the thermocline, which will be constrained by our assumption of uniform potential vorticity. This is done in the next section.

b. *The thermocline*

We suppose that the moving waters of the thermocline are divided from the motionless abyss by the "bowl" $z=-D(x, y)$. Density is assumed to be continuous across this bowl.

Outside and on the bowl the stratification takes up its reference state denoted by subscript zero (see Fig. 1):

$$\rho=\rho_0(z);\quad z=z_0(\rho) \quad (8)$$

as does the pressure

$$p=p_0(z)=g\int_z^0\rho_0(z)dz. \quad (9)$$

So, equating the pressure on the bowl to the reference pressure, by hydrostasy

$$p_s+g\int_{-D}^{0}\rho(x, y, z)dz=g\int_{-D}^{0}\rho_0 dz$$

and integrating by parts and then reexpressing in terms of ρ,

$$p_s(x, y)=-g\left\{\int_{\rho_m}^{\rho_D}z(\rho, x, y)d\rho-\int_{\rho_{m0}}^{\rho_D}z_0(\rho)d\rho\right\} \quad (10)$$

where $\rho_D(x, y)=\rho_0(-D)$ is the density on the bowl. We have thus related the surface pressure field, and hence mixed-layer velocity field, to the density structure in the thermocline.

Now the geostrophic velocity in the thermocline can be expressed as

$$\mathbf{u}=\frac{1}{\bar{\rho}f}\mathbf{k}\times\nabla_\rho M'$$

where $\nabla_\rho=\mathbf{i}(\partial/\partial x)|_{\rho=\text{const}}+\mathbf{j}(\partial/\partial y)|_{\rho=\text{const}}$, and the perturbation Montgomery potential follows from the density structure by

$$M'(\rho, x, y)=-g\int_{\rho}^{\rho_D}\{z(\rho, x, y)-z_0(\rho)\}d\rho. \quad (11)$$

Equations (10) and (11) are completely general; in the following paragraphs we specialize them to the case where the potential vorticity within the moving thermocline is uniform.

We now hypothesize that everywhere in the moving thermocline, potential vorticity is specified as a function of Montgomery function and density: $Q\equiv Q(M', \rho)$. For analytical convenience and hence clarity of exposition, we suppose it to be uniform on each isopycnal, *even on surfaces that outcrop:* $Q\equiv -f\bar{\rho}^{-1}\partial\rho/\partial z=Q_0(\rho)$. In particular, we choose

$$Q_0(\rho)=-f_0\bar{\rho}^{-1}\frac{\partial\rho_0}{\partial z}; \quad (12)$$

that is, the value to which Q is homogenized on *every* surface is the value appropriate to the reference stratification at $f=f_0$, defined here as the zero wind stress curl line. Thus,

$$\frac{\partial z}{\partial\rho}=\frac{f}{f_0}\frac{\partial z_0}{\partial\rho}. \quad (13)$$

The ratio of the actual isopycnal layer thickness to the reference layer thickness—the thickness ratio—is independent of depth and equal to f/f_0: isopycnals are

squashed together in a subtropical gyre but pulled apart in the subpolar gyre.

Because the thickness ratio is independent of depth, we may integrate (13) up from the bowl $z = -D$ to give the position of an isopycnal in the thermocline $z(\rho)$ expressed in terms of its reference position $z_0(\rho)$ and D. Thus,

$$z + D = \frac{f}{f_0}(z_0 + D). \tag{14}$$

Furthermore, h and D are related through

$$D - h = \frac{f}{f_0}(D - h_0) \tag{15}$$

where $h_0 = -z_0(\rho_m)$. Equations (14) and (15) have been derived before: see Marshall and Nurser (1988) and Nurser (1988), where they have been used to interpret observations of the Gulf Stream. In the present context, however, they tell us that if any two of D, h, and ρ_m are known, then the other can be found from (15) and the whole structure of the thermocline can be deduced. In particular, using (14) to eliminate z from the expression (10) for the surface pressure field allows it to be expressed

$$p_s(D, \rho_m, f) = -g\left\{\int_{\rho_m}^{\rho_D}\left(\frac{f}{f_0}z_0(\rho) + D\left(\frac{f}{f_0} - 1\right)\right)d\rho - \int_{\rho_{m_0}}^{\rho_D} z_0(\rho)d\rho\right\}. \tag{16}$$

Our knowledge of the potential vorticity field has reduced the problem to the determination of two fields, D and ρ_m, say. Two constraints are needed to determine the two fields. These are provided here by the mixed-layer thermodynamic equation (7) and the Sverdrup constraint for the depth-integrated flow, described in the next section.

Note that a specification of $Q \equiv Q(M', \rho)$ leads (see Huang 1988a) to a second order ODE for M' in terms of ρ, rather than the simple first-order expression for z, (13). Integration of this second-order ODE gives (rather more complicated) expressions for $z(\rho, D)$ and $h(\rho_m, D)$ analogous to (14) and (15), but the thermocline structure is once more completely set by the two fields D and ρ_m.

c. *The Sverdrup constraint*

As long as the bowl does not strike the ocean floor, $w = 0$ at $z = -D$, and the depth-integrated geostrophic flow is constrained by the Ekman suction $w_e = \mathbf{k} \cdot \nabla \times (\tau/f\bar{\rho})$;

$$\beta \int_{-D}^{0} v dz = f w_e. \tag{17}$$

The geostrophic flow is linked to the hydrography by thermal wind. But, because potential vorticity is uniform, the hydrography is completely determined by D and ρ_m. Hence, the Sverdrup relation provides the second required constraint relating D and ρ_m.

Here we reformulate the Sverdrup constraint in terms of the depth integral of the pressure, which can be elegantly linked to the density structure—the hydrography. Consider the depth integral of the perturbation pressure

$$P' = \int_{-D}^{0} \{p(x, y, z) - p_0(z)\} dz. \tag{18}$$

Contours of constant P' are streamlines of the depth-integrated flow; in the f-plane limit $P'/(f\bar{\rho})$ is the streamfunction for the depth-integrated geostrophic flow.

In terms of P', the Sverdrup constraint (17) takes the form

$$\frac{\beta}{\bar{\rho}f}\frac{\partial P'}{\partial x} = f w_e.$$

So, on a β plane, supposing that $P' = P'_E$ is known at the eastern boundary $x = x_E$,

$$P' = \int_{x_E}^{x} \frac{\bar{\rho}f^2 w_e}{\beta} dx + P'_E.$$

In terms of the spherical polars used to produce the results of section 4, we have

$$P' = \int_{\lambda_E}^{\lambda} \frac{\bar{\rho}f^2 w_e}{\beta} R\cos\theta d\lambda + P'_E, \tag{19}$$

where λ and θ are longitude and latitude, respectively, $R = 6370$ km is the radius of the earth, and $\lambda = \lambda_E$ is the eastern boundary, along which the pressure is P'_E. The pressure field for the depth-integrated flow is determined by the Ekman pumping field, together with an appropriate eastern boundary condition—P' is *imposed* by the Sverdrup constraint.

We wish to link the depth-integrated perturbation pressure field P' to the density field.

Consider the actual and reference pressure parts of the definition (18) separately. Consider first the actual pressure integral. Integrating by parts and using hydrostasy,

$$\int_{-D}^{0} p dz = [pz]_{-D}^{0} + \int_{-D}^{0} \rho z g dz,$$

and integrating by parts a second time

$$\int_{-D}^{0} p dz = \left[pz + \frac{g}{2}\rho z^2\right]_{-D}^{0} - \frac{g}{2}\int_{-D}^{0} z^2 \frac{\partial \rho}{\partial z} dz.$$

Treating the integral of the reference pressure similarly, noting that pressure and density return to their reference values on the bowl, yields

$$P' = \frac{g}{2}\left\{\int_{\rho_m}^{\rho_D} z^2(\rho, x, y)d\rho - \int_{\rho_{m0}}^{\rho_D} z_0^2(\rho)d\rho\right\}. \tag{20}$$

Here, as before, z and z_0 are the actual and reference positions of the isopycnals, with ρ_m and ρ_{m0} the actual and reference values of the surface density. The integral $\frac{1}{2}g\int z^2 d\rho$ is the continuous representation of the $\frac{1}{2}\bar{\rho}\sum_i g_i' h_i^2$ form for the depth-integrated pressure that appears in the layered models (e.g., Luyten et al. 1983).

Equation (20) is quite general and makes no assumption about the interior potential vorticity field. Since P' is fixed by the imposed Ekman pumping field, Eqs. (19) and (20) provide a constraint on the hydrography. The immediate elimination of P' between (19) and (20) leads to a formula similar to that obtained by Huang (1989) and Williams (1989). The thermocline models of these authors use this to help *find* the potential vorticity distribution.

However, we *know* the potential vorticity distribution; thus, the density structure $z(\rho, x, y)$ is given by (14) and (15) in terms of D, ρ_m, and the *known* field f/f_0. Substituting (14) and (15) into (20),

$$P' \equiv P'(D, \rho_m, f) = \frac{g}{2}\left\{\int_{\rho_m}^{\rho_D}\left[\frac{f}{f_0}z_0(\rho) + D\left(\frac{f}{f_0} - 1\right)\right]^2 d\rho - \int_{\rho_{m0}}^{\rho_D} z_0^2(\rho)\,d\rho\right\}. \quad (21)$$

Thus, P' depends only on D and ρ_m (and f/f_0). But P' is known independently from the Sverdrup constraint (19). Hence,

$$D \equiv D(P', \rho_m, f) \equiv D(\rho_m, x, y).$$

If ρ_m is prescribed, as in Pedlosky and Young (1985) or Nurser (1988), the problem is solved; we iterate (21) to find the D that gives the correct value of P', and then use (14) to find the density field. In the present model, however, we first have to find ρ_m; the method of solution involves the mixed-layer thermodynamic equation and is described in the next section.

3. Method of Solution

a. *Transformation of the thermodynamic equation*

The steady thermodynamic equation (7)

$$\frac{1}{\bar{\rho}f}\mathbf{k}\times\nabla p_s\cdot\nabla\rho_m = -\frac{\alpha_E\mathscr{H}_{\text{net}}}{hc_W}$$

is now transformed into a single equation in ρ_m. We do this by reformulating the advection term in the quasi-linear form $\mathbf{u}_c\cdot\nabla\rho_m$ where the characteristic velocity $\mathbf{u}_c$ at each point can be calculated from the values of ρ_m at that point only. In order to do this we use the fact that we know $p_s \equiv p_s(D, f, \rho_m) \equiv p_s(\rho_m, x, y)$ from (16) and (21).

We find (details appear in the appendix) that (7) can be written

$$\left.\begin{aligned}\mathbf{u}_c\cdot\nabla\rho_m &= -\frac{\alpha_E\mathscr{H}_{\text{net}}}{hc_W}\\ \text{where the characteristic velocity } \mathbf{u}_c \text{ is}&\\ \mathbf{u}_c &= (A\mathbf{k}\times\nabla P' + B\mathbf{k}\times\nabla f)/(\bar{\rho}f)\end{aligned}\right\} \quad (22)$$

and the coefficients A and B in (22) are

$$A = \frac{1}{D - \alpha I_1/I_0} \quad (23)$$

and

$$B = \frac{\alpha I_1}{f_0}\frac{I_1/I_0 - I_2/I_1}{D - \alpha I_1/I_0} \quad (24)$$

where $\alpha = f/f_0$ and

$$I_0 = I_0(D, \rho_m) = g\int_{\rho_m}^{\rho_D} d\rho$$

$$I_1 = I_1(D, \rho_m) = g\int_{\rho_m}^{\rho_D} (D + z_0)\,d\rho$$

$$I_2 = I_2(D, \rho_m) = g\int_{\rho_m}^{\rho_D} (D + z_0)^2\,d\rho.$$

Hence, $A \equiv A(\rho_m, D, f)$ and $B \equiv B(\rho_m, D, f)$, from which D can be eliminated in favor of P', f, and ρ_m using (21). Thus, $\mathbf{u}_c \equiv \mathbf{u}_c(\rho_m, x, y)$, the x and y dependence arising from the known spatial variation of P' and f. Similarly h, which is by (15) a function of ρ_m and D, also reduces to a function of ρ_m, x, and y.

Thus, as long as $\mathscr{H}_{\text{net}} \equiv \mathscr{H}_{\text{net}}(\rho_m, x, y)$, (22) is one equation in one unknown ρ_m. It should be noted that $\mathscr{H}_{\text{net}}$ is not the surface heating $\mathscr{H}_{\text{in}}$, but rather, (4), the surface heating less the advection by the Ekman flux, which is of comparable magnitude. Should we so wish, (4) could be used to eliminate $\mathscr{H}_{\text{net}}$ from (22), yielding

$$\left(\mathbf{u}_c + \frac{1}{h\bar{\rho}f}\mathbf{k}\times\boldsymbol{\tau}\right)\cdot\nabla\rho_m = -\frac{\alpha_E\mathscr{H}_{\text{in}}}{hc_W},$$

and the model is thus driven by $\mathscr{H}_{\text{in}}$. However, for simplicity, in the solutions presented in the next section we choose to specify $\mathscr{H}_{\text{net}}$ and use (22).

The characteristic velocity is built up of $A\mathbf{k}\times\nabla P'$ and $B\mathbf{k}\times\nabla f$ terms. The $A\mathbf{k}\times\nabla P'$ term is the mixed-layer velocity expected if the slope of the isopycnals within the bowl did not vary with depth. Because potential vorticity is uniform within the bowl, this is true for the *zonal* slope. The $B\mathbf{k}\times\nabla f$ term is an eastward correction, which arises from the thickening of the isopycnals toward the north required to assure uniformity of potential vorticity.

Where the mixed layer has a horizontal temperature gradient (and hence vertical velocity shear), $\mathbf{u}_c$ can be shown to be equal to the velocity at a point lying between the base and the midpoint ($z = -h/2$) of the mixed layer.

Luyten and Stommel (1986a,b) and Veronis (1988) transformed the thermodynamic equation for a model with two active layers constrained to be in Sverdrup balance into a form very similar to (22). In their simpler problem they were able to interpret the characteristic velocity as that of a Rossby wave suffering advection by the Sverdrup flow.

b. *Integration of the characteristic equation*

If ρ_m is known along a curve that crosses the characteristics, we can integrate along the characteristics to find the ρ_m field. In the runs described in section 4, ρ_m has simply been specified on the boundary of the domain of interest wherever the characteristic velocity is inward. We integrate inward along the characteristics and interpolate to find the ρ_m field everywhere. The D field and the rest of the solution then follow. The domain has been chosen such that all characteristics originate from the boundary, so there are no closed characteristics.

In more detail, we integrate along characteristics as follows:

(i) at our starting point $(x, y) = \mathbf{x} = \mathbf{x}^0$, we know $\rho_m = \rho_m{}^0$ (say);
(ii) we calculate $\mathbf{u}_c$, h and $\mathscr{H}_{\text{net}}$;
(iii) then at the next point on the characteristic curve

$$\mathbf{x}^1 = \mathbf{x}^0 + \Delta t\, \mathbf{u}_c$$

where

$$\rho_m{}^1 = \rho_m{}^0 - \Delta t\, \alpha_E \mathscr{H}_{\text{net}}/(hc_W).$$

Step (ii) is then repeated using the new values $\mathbf{x}^1$ and $\rho_m{}^1 \ldots$. The integration (which is actually performed by a fourth-order Runge–Kutta scheme) is carried on until we pass out of the domain of interest.

In order to calculate $\mathbf{u}_c$ and h, we need first to find D from ρ_m, x, and y. We do this by iterating (21) by a Newton–Raphson method to find the value of D, which, for given values of ρ_m and f, gives the correct value of P'. Then h is immediately given by (15). The fields of $\nabla P'$ and ∇f are known, so we simply need the coefficients A and B in order to evaluate $\mathbf{u}_c$.

Note that, because (22) is a quasi linear, if unsuitable ρ_m values are specified at the boundaries, the characteristics may cross or fail to cover the domain of interest (Luyten and Stommel 1986c; Veronis 1988).

4. Some idealized experiments

a. *The subtropical gyre*

Note that all results have been calculated using full spherical geometry, and so are presented in terms of longitude λ and latitude θ. We suppose the subtropical gyre to fill the region $\lambda_W < \lambda < \lambda_E$; $\theta_S < \theta < \theta_N$, with $\lambda_W = -80°$, $\lambda_E = -20°$; $\theta_S = 15°$, $\theta_N = 40°$.

Within this region we apply a sinusoidally varying Ekman pumping field:

$$w_e = w_e^* \sin\left(\frac{\pi(\theta - \theta_S)}{\theta_N - \theta_S}\right), \tag{25}$$

with a maximum Ekman pumping $w_e^* = -1.5 \times 10^{-6}$ m s^{-1} $\approx$ 47 m yr^{-1}. It is plotted in Fig. 2a. The depth-integrated flow follows contours of the depth-integrated perturbation pressure, which is set by the Sverdrup constraint (19), so

$$P' = -\frac{\bar{\rho} f^2 R \cos\theta}{\beta}(\lambda - \lambda_E) w_e(\theta). \tag{26}$$

We have specified $P' \equiv 0$ at the eastern boundary, thus, forbidding any barotropic flow across it.

Contours of P' are plotted in Fig. 2b. The total southward geostrophic flow across a line of latitude is $P'/\bar{\rho}f$: This reaches a maximum of ~30 Sv (Sv $\equiv 10^6$ m^3 s^{-1}), representing the transport of the gyre.

1) BOUNDARY CONDITIONS

We wish to ensure that the flow is confined within the gyre; that is, there is no zonal flow across the eastern boundary at any depth. This is only consistent [see

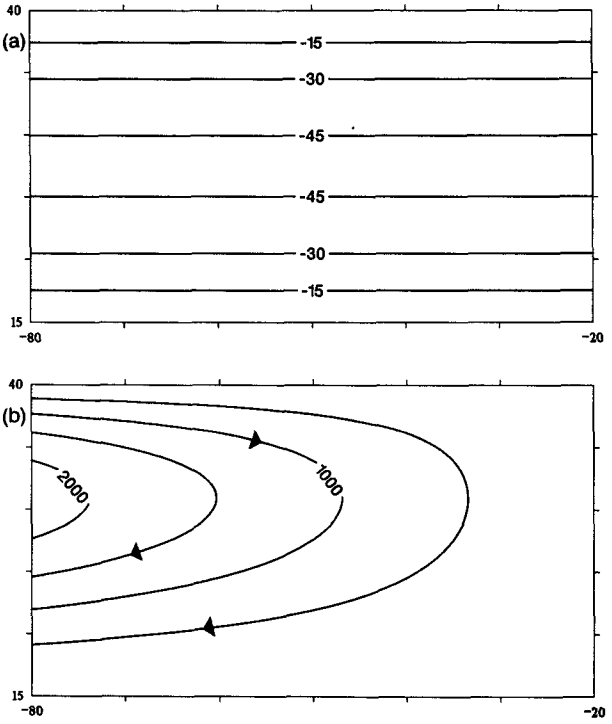

FIG. 2. The forcing applied to the subtropical gyre. The model subtropical basin extends from 15° to 40°N and from 80° to 20°W. (a) Contours of Ekman suction in meters per year. (b) Contours of the depth-integrated perturbation pressure, P', units: 10^3 N m^{-1}.

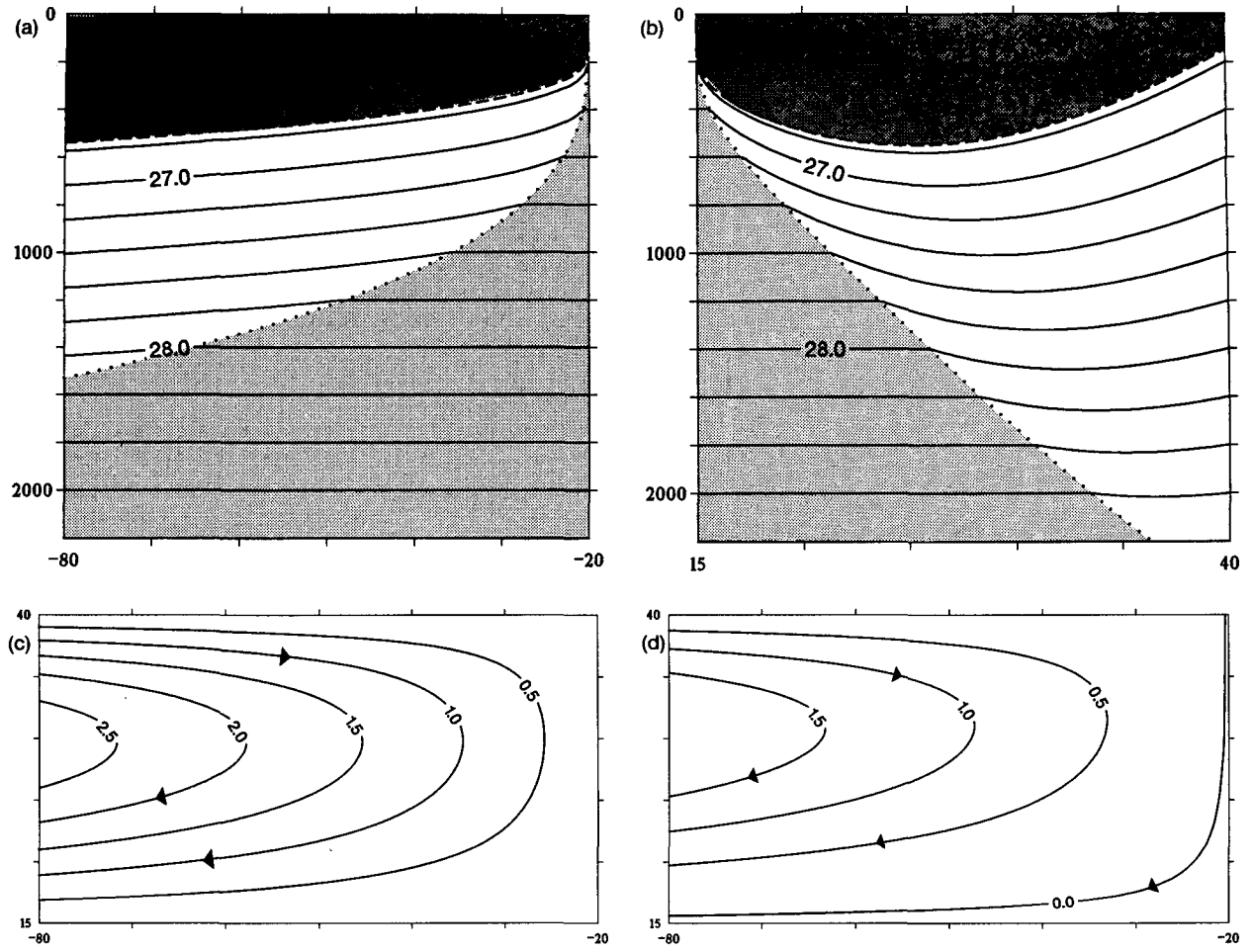

FIG. 3. A subtropical gyre with mixed layer of uniform density, $\sigma = 26.75$. (a) A zonal cross section at latitude 27.5°N, halfway up the gyre. The mixed layer is stippled heavily, the moving thermocline left blank, and the motionless abyss stippled lightly. Isopycnals are plotted every 0.2 kg m^{-3}. (b) A meridional cross section at longitude 80°W, on the western edge of the gyre. Notation as in (a). (c) Contours of the surface pressure field, p_s, units: 10^3 N m^{-2}. (d) Contours of the Montgomery function on the isopycnal surface $\sigma = 27.0$, units: 10^3 N m^{-2}.

(21)] with the vanishing of the perturbation pressure, $P_E = 0$, if the mixed-layer density reaches its reference value, $\rho_m = \rho_{m0}$, on the eastern boundary. Care must be taken to ensure that the inflow condition on the western boundary and any applied thermal forcing are consistent with this requirement.

2) THE REFERENCE STRATIFICATION

For convenience we choose the linear reference stratification

$$\rho_0(z) = 1026.6 - 10^{-3}z. \qquad (27)$$

This is a uniform density gradient of 1 kg m^{-3}/km. For these subtropical runs we choose a reference mixed-layer density—the density of the mixed layer on the eastern boundary—of $\rho_{m0} = 1026.75$, which implies that the "reference thickness" of the mixed layer $H_0 = -z_0(\rho_{m0}) = 150$ m.

3) A MIXED LAYER OF SPECIFIED UNIFORM DENSITY

We first adopt a mixed layer whose density is everywhere uniform and is equal to its reference value; this is the case treated by Pedlosky and Young (1983) and by Nurser (1988). Thus, $\rho_m(\lambda, \theta) \equiv \rho_{m0} = 1026.75$. Since ρ_m is known, the bowl depth D follows immediately from (21), with P' given by the Sverdrup constraint (26). Fields of z, M', and p_s then follow from (14), (11), and (10), respectively.

Everywhere inside the bowl the isopycnals dip toward the west to accommodate the southward Sverdrup transport (see the zonal section Fig. 3a). Because po-

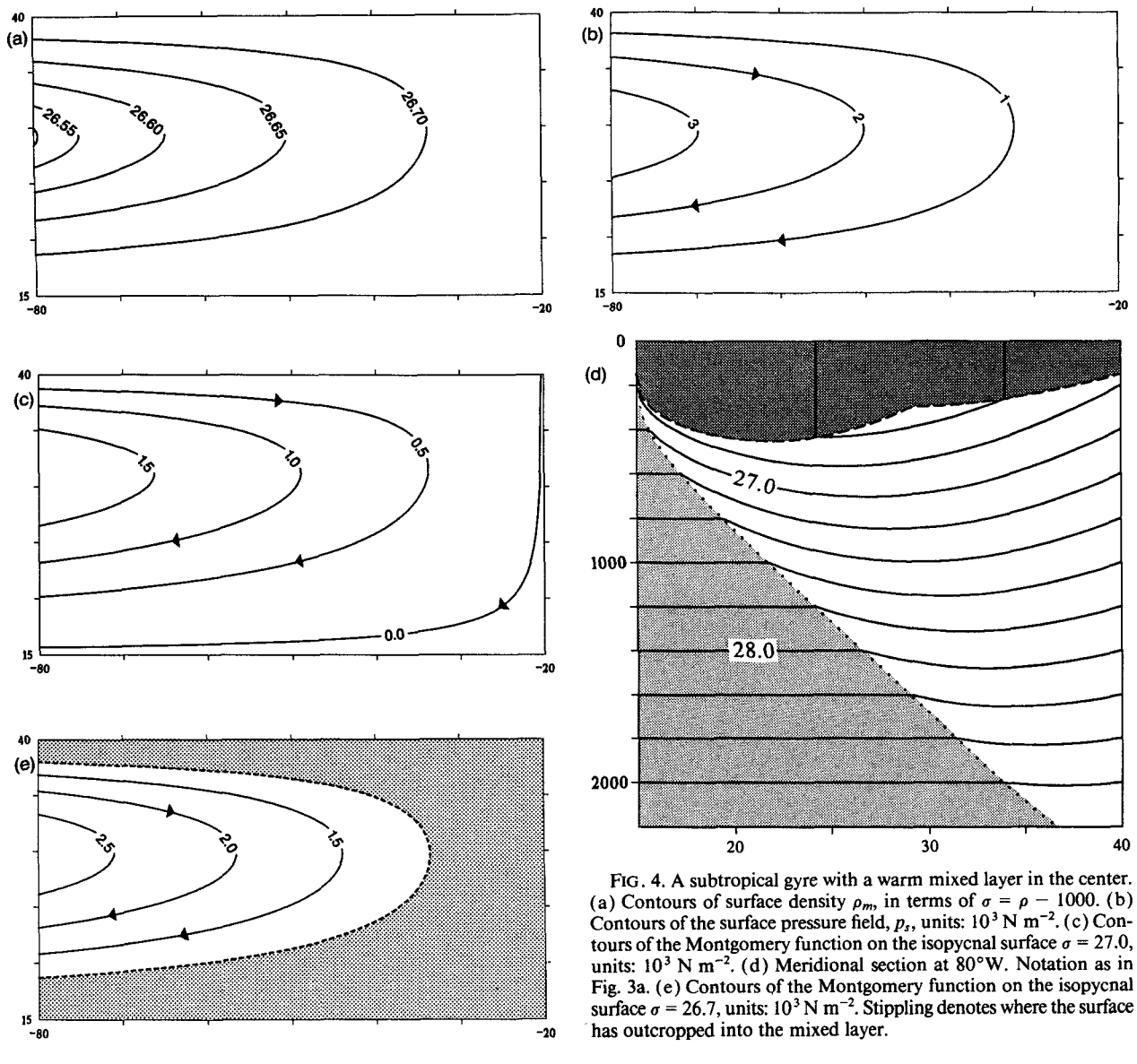

FIG. 4. A subtropical gyre with a warm mixed layer in the center. (a) Contours of surface density ρ_m, in terms of $\sigma = \rho - 1000$. (b) Contours of the surface pressure field, p_s, units: 10^3 N m^{-2}. (c) Contours of the Montgomery function on the isopycnal surface $\sigma = 27.0$, units: 10^3 N m^{-2}. (d) Meridional section at 80°W. Notation as in Fig. 3a. (e) Contours of the Montgomery function on the isopycnal surface $\sigma = 26.7$, units: 10^3 N m^{-2}. Stippling denotes where the surface has outcropped into the mixed layer.

tential vorticity is uniform in the thermocline, their slope is independent of depth. In particular, the $\sigma = 26.75$ isopycnal (here σ is simply given by $\rho - 1000$), which marks the base of the mixed layer, must slope down: the mixed layer thickens toward the west.

The meridional section in Fig. 3b shows, with little difference from Fig. 7a of Rhines and Young (1982), the poleward deepening of the bowl so characteristics of the observations. As f tends to f_0 and hence $\partial\rho/\partial z$ within the bowl tends to $\partial\rho_0/\partial z$, D must increase in order to ensure substantial downward deviation of the isopycnals and increasing depth-integrated pressure.

The surface pressure field and the Montgomery function on the $\sigma = 27.0$ surface are plotted in Figs. 3c and 3d, respectively.

Note that *all* of the Ekman pumping is absorbed into the mixed layer. There is *no* ventilation of the stratified thermocline in this steady model.

4) WARM MIXED LAYER IN THE CENTER OF THE GYRE

The thermodynamic equation is now used to set the density of the mixed layer by advecting in the density field from values set at the boundary of the domain. There is no diabatic heating. The characteristics that advect the mixed-layer density field are, as we shall see, dominated by the Sverdrup flow. It is thus the inflow condition along the northern part of the western boundary of the half-disk that sets the density field.

Note that the inflow condition sets the mixed-layer density field only on that part of the western boundary through which inflow is taking place.

Suppose a density inflow condition

$$\rho_m = 1026.75 - .025 \times (40 - \theta^0) \qquad (28)$$

that becomes less dense (i.e., warmer) to the south. A warm mixed layer (Fig. 4a) is advected into the center of the gyre. Since the model is adiabatic, the characteristics coincide with contours of the mixed-layer density. They are pushed eastward a little from the streamlines P' of the barotropic flow by the ∇f term.

The warm pool in the center of the gyre implies, by thermal wind, anticyclonic shear throughout the mixed layer. This drives a surface flow considerably stronger (Fig. 4b) than would occur (Fig. 3c) if the mixed layer were of uniform density. On the other hand, the flow in the thermocline is weakened; compare Fig. 4c, the flow pattern on the $\sigma = 27.0$ surface (reference depth 400 m), with Fig. 3d, the corresponding flow pattern when the mixed layer is uniform. This weaker flow is associated with a somewhat shallower bowl; compare the meridional section at 80°W (Fig. 4d) with the corresponding section (Fig. 3b) for the case with uniform mixed-layer density. Why is the bowl now shallower than in the reference solution?

The response of the depth of the bowl to a change in the density of the mixed layer is given by differentiating (21) by ρ_m and D and combining the resulting equations to yield

$$\left.\frac{\partial D}{\partial \rho_m}\right|_{P',f=\text{const}} = -\left(\frac{\partial P'}{\partial \rho_m}\right)\Big/\left(\frac{\partial P'}{\partial D}\right) = \frac{\frac{1}{2}h^2}{(1 - f/f_0)\int_{\rho_m}^{\rho_D}\{-z\}\,d\rho}. \qquad (29)$$

In the subtropical gyre $f/f_0 < 1$; as $z < 0$, the denominator is positive. Thus, if the mixed layer becomes warmer, then the bowl must shoal (and vice versa). The magnitude of $\partial D/\partial \rho_m$ lies generally in the range 200–1000 m/kg m^{-3} for the runs described here. The bowl depth is therefore little affected by mixed-layer density variations of order 0.1 kg m^{-3} as chosen here.

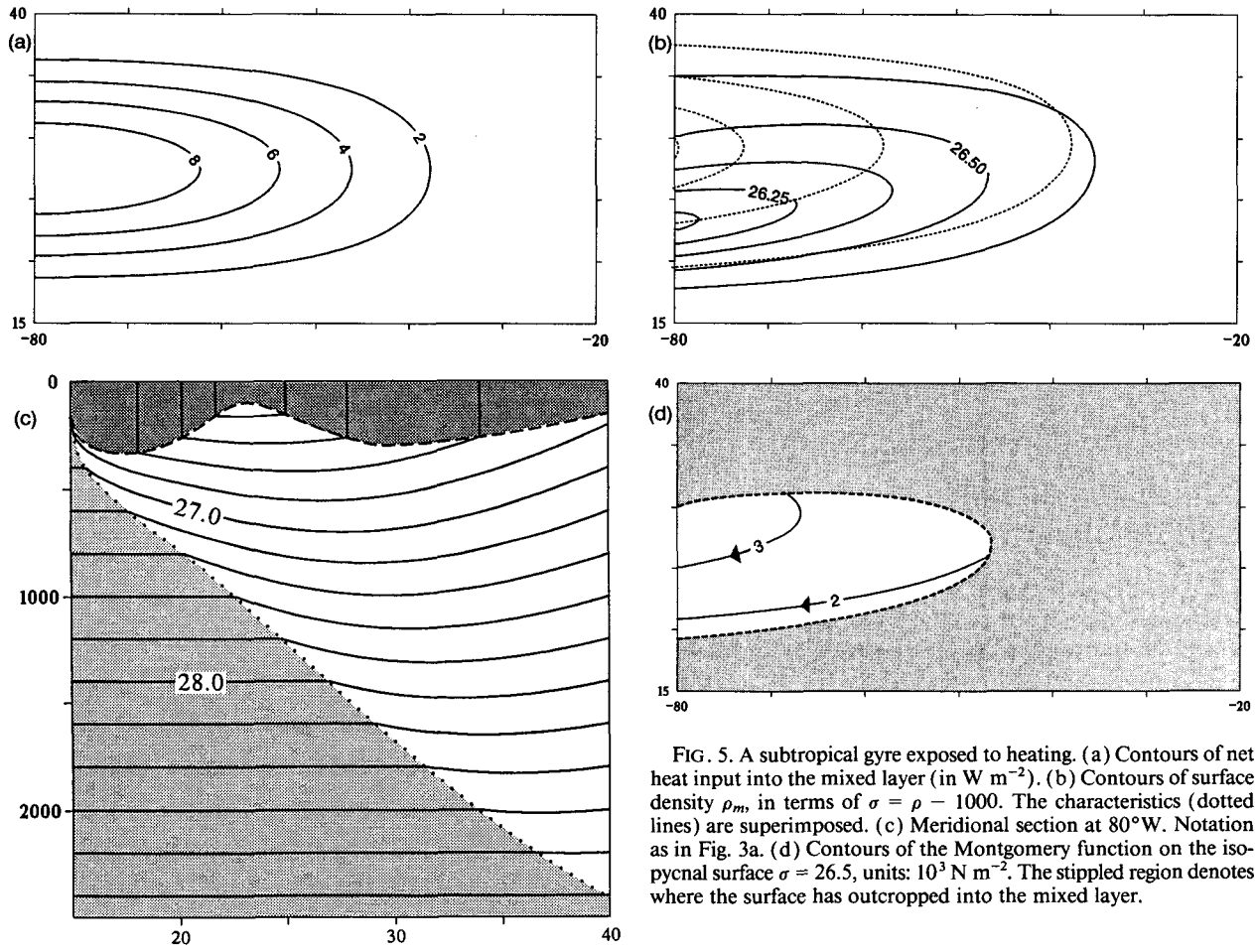

FIG. 5. A subtropical gyre exposed to heating. (a) Contours of net heat input into the mixed layer (in W m^{-2}). (b) Contours of surface density ρ_m, in terms of $\sigma = \rho - 1000$. The characteristics (dotted lines) are superimposed. (c) Meridional section at 80°W. Notation as in Fig. 3a. (d) Contours of the Montgomery function on the isopycnal surface $\sigma = 26.5$, units: 10^3 N m^{-2}. The stippled region denotes where the surface has outcropped into the mixed layer.

It should be noted that now isopycnals outcrop into the mixed layer; however, there is no transfer of fluid *between* the mixed layer and the thermocline. This is evident in, for example, the flow on the outcropping $\sigma = 26.7$ surface (Fig. 4e). The reason that ventilation does not occur is that (see NM) no net diabatic heating is applied to the mixed layer: $\mathscr{H}_{\text{net}} \equiv 0$.

5) WARMING OF THE SUBTROPICAL GYRE

The mixed layer is now diabatically warmed by the net heating field (Fig. 5a)

$$\mathscr{H}_{\text{net}} = \mathscr{H}^*_{\text{net}} \sin^2\left(\frac{\pi(\theta - \theta_S)}{\theta_N - \theta_S}\right) \cos\left(\frac{\pi(\lambda - \lambda_W)}{\lambda_E - \lambda_W}\right) \quad (30)$$

where the maximum heating rate $\mathscr{H}^*_{\text{net}} = 10$ W m^{-2}. We choose the inflow condition (28), which is warmer to the south as in the previous example.

The heating causes the density to decrease along characteristics (the dotted lines in Fig. 5b). The tongue of low-density water in the southwest corner marks the water that has a long track over the region of strong warming. Note that density does not vary along the characteristic originating from the western boundary at 40°N, a consequence of the form (30) of the heating. Where the mixed layer has been warmed it shoals and, to a lesser extent, (see the meridional section Fig. 5c), so does the bowl.

As a consequence of the applied heating, there is now transfer of fluid from the mixed layer into the thermocline. This "subduction" is evident in Fig. 5d, the plot of Montgomery function on the $\sigma = 26.5$ surface. It is also clear in Fig. 6, the perspective plot of this same surface; fluid spirals down on the $\sigma = 26.5$ surface, leaving the mixed layer along the outcrop line.

We refer the reader to NM for more discussion of the processes that set the rate at which fluid passes into the thermocline.

b. *The subpolar gyre*

We now apply the model to a subpolar gyre: $\lambda_W < \lambda < \lambda_E$; $\theta_S < \theta < \theta_N$, with λ_W and λ_E as before, but now $\theta_S = 40°$, $\theta_N = 65°$. An Ekman suction is imposed of exactly the same form and strength as (25) but opposite sign.

Potential vorticity in the thermocline is now assumed to be homogenized to its reference value on the southern edge of the gyre. To model the thicker mixed layer observed in the subpolar gyre, a reference mixed-layer

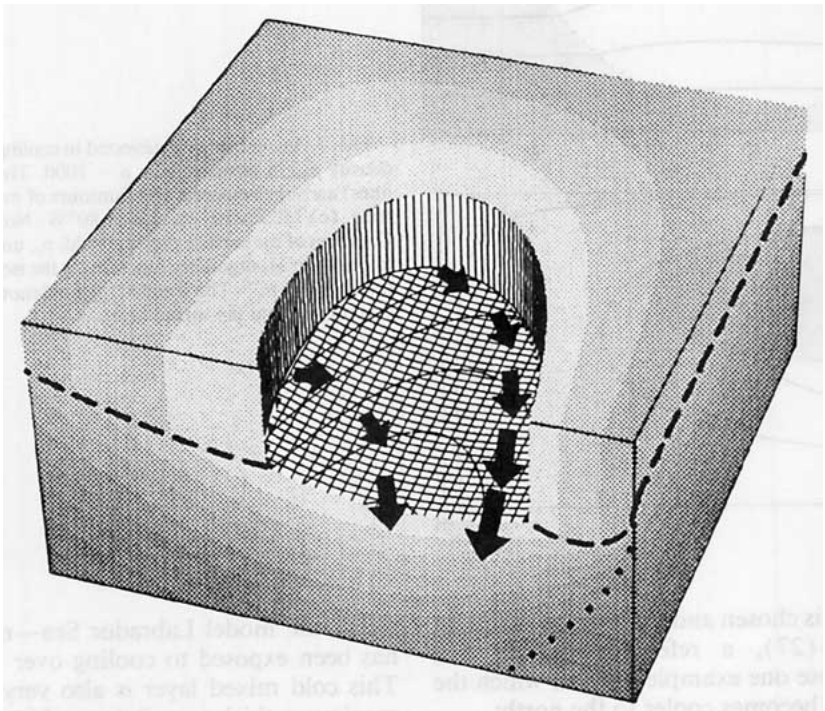

FIG. 6. A perspective plot of the upper 800 m of the subtropical gyre, viewed from the southwest. The $\sigma = 26.5$ surface appears as a net; its depth is contoured every 25 m. The velocities on this surface are proportional to the length of the arrows. The "wall" denotes where the $\sigma = 26.5$ surface outcrops into the mixed layer.

A grey scale is used to represent the density field, both on the surface of the mixed layer and on the vertical planes. Each element of the grey scale covers a density range of 0.1 kg m^{-3}. The mixed-layer base is delineated by a dashed line, and the "bowl" by the dotted line.

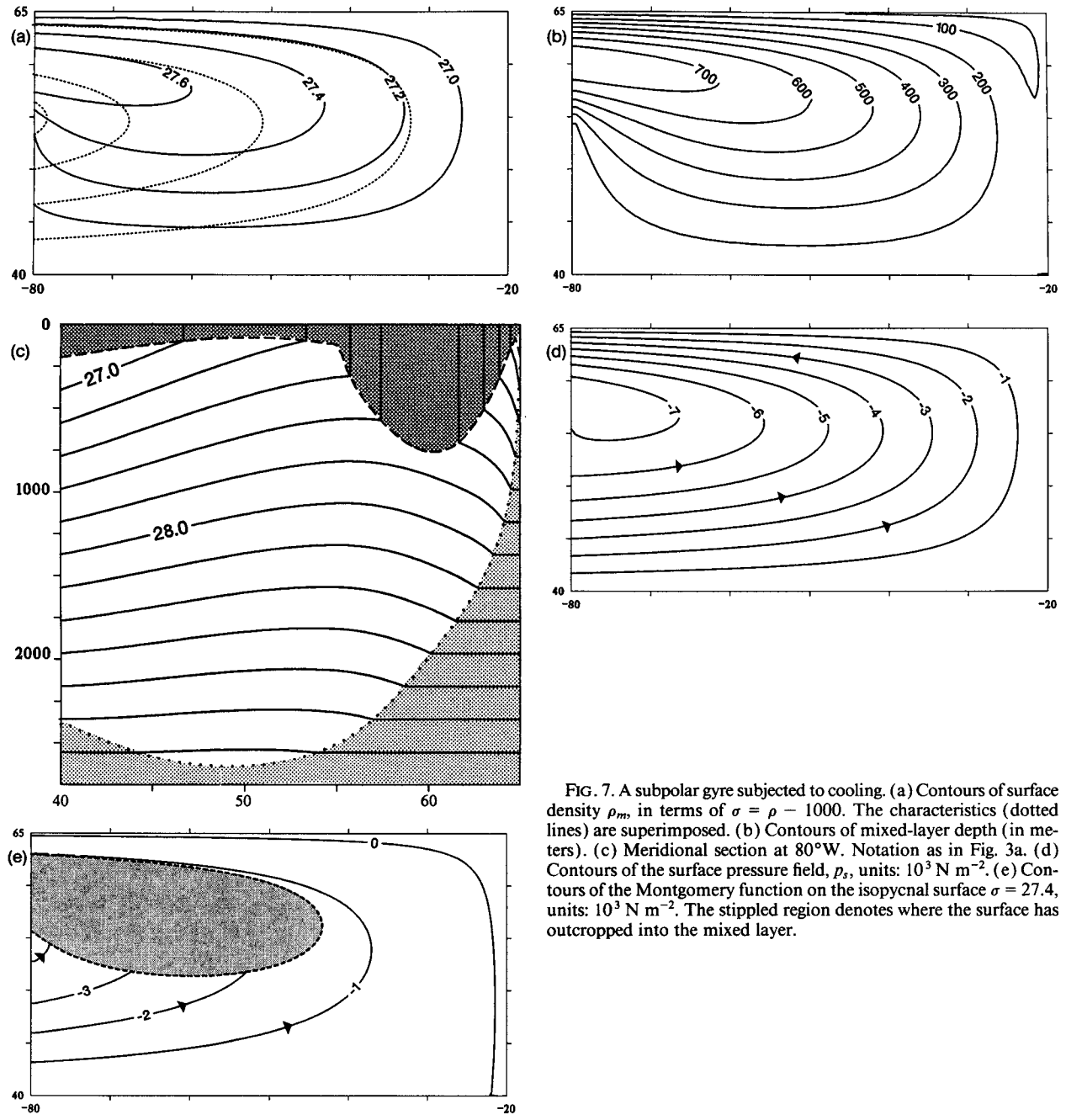

FIG. 7. A subpolar gyre subjected to cooling. (a) Contours of surface density ρ_m, in terms of $\sigma = \rho - 1000$. The characteristics (dotted lines) are superimposed. (b) Contours of mixed-layer depth (in meters). (c) Meridional section at 80°W. Notation as in Fig. 3a. (d) Contours of the surface pressure field, p_s, units: 10^3 N m^{-2}. (e) Contours of the Montgomery function on the isopycnal surface $\sigma = 27.4$, units: 10^3 N m^{-2}. The stippled region denotes where the surface has outcropped into the mixed layer.

thickness of 200 m is chosen and, in order to maintain consistency with (27), a reference density $\rho_{m0} = 1026.8$. We choose one example only, in which the mixed-layer inflow becomes cooler to the north:

$$\rho_m = 1026.8 + .03 \times (\theta^0 - 40),$$

and the mixed layer is subjected to a net cooling of the same form as (30) but now $\mathscr{H}^*_{\text{net}} = -40$ W m^{-2}.

Standing out in the surface density field (Fig. 7a) is the tongue of high-density water lying to the northwest—the model Labrador Sea—marking water that has been exposed to cooling over a prolonged track. This cold mixed layer is also very thick, attaining a maximum thickness of almost 800 m—see the mixed-layer thickness field (Fig. 7b) and the meridional section (Fig. 7c).

The upward doming of the isopycnals toward the center of the gyre, necessary to generate the cyclonic depth-integrated flow, is evident in the meridional section (Fig. 7c). The increasingly dense fluid on the

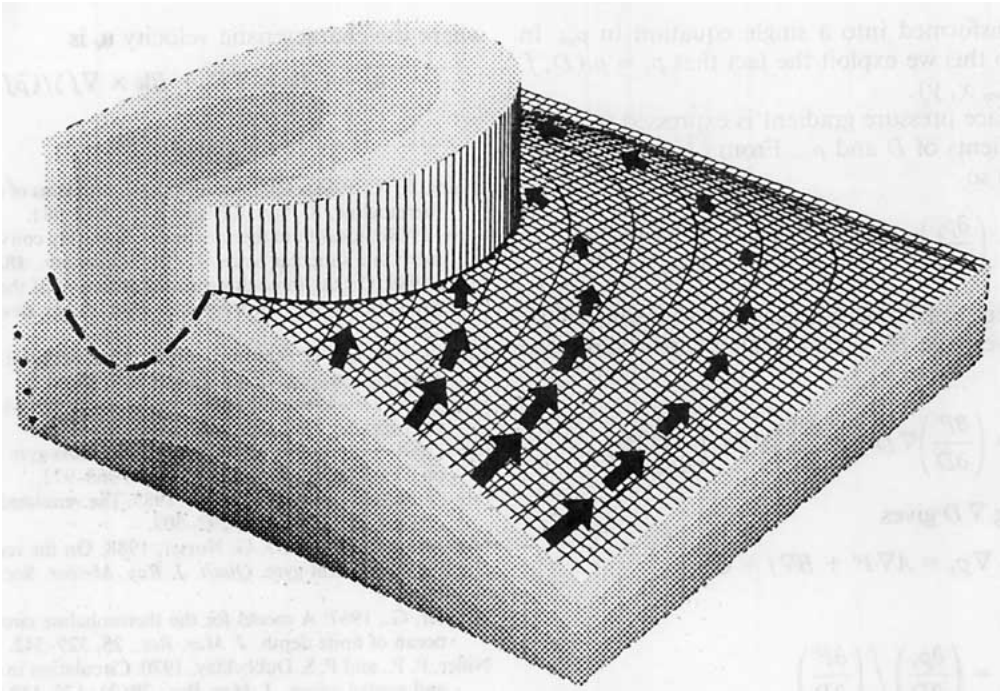

FIG. 8. A perspective view of the upper 1200 m of the subpolar gyre, viewed from the southwest. The $\sigma = 27.4$ surface appears as a net, and its depth contoured every 50 m. Grey scale interval is again 0.1 kg m^{-3}.

northern flank of the inflow prevents the mixed layer from surfacing, but cannot prevent a slight shallowing toward the center of the gyre (Figs. 7b and 7c).

The surface flow (Fig. 7d) is intensified by the cyclonic shear in the mixed layer. More interesting is the flow in the thermocline; Fig. 7e shows contours of M' on the $\sigma = 27.4$ surface. Note the entrainment of fluid into the mixed layer: Fluid flowing along this constant density surface runs into the mixed layer where it has cooled enough to burrow down across this density surface.

The upward spiraling of fluid, until it strikes the downward burrowing mixed layer, is clear in the perspective diagram of the $\sigma = 27.4$ surface (Fig. 8). This transfer of fluid into the mixed layer from the thermocline, a consequence of the applied cooling field, is discussed in more detail in NM.

5. Conclusions

We have shown how to formulate and find solutions for a steady ideal thermocline underlying a vertically homogeneous mixed layer exposed to mechanical and thermodynamic forcing. The mathematical elegance and tractability of our model follows from the simplifying assumption that the potential vorticity of the thermocline has a uniform unchanging value. This allows us to drive the model with nontrivial patterns of wind and thermal forcing and permits a mixed layer whose depth and temperature vary both with latitude and longitude. The surface temperature is found rather than prescribed.

In a companion paper, Nurser and Marshall (1991), we employ the model to study those factors that control the magnitude and sense of flow between the mixed layer and the thermocline.

The model can be generalized to accommodate a potential vorticity that is a function of both Montgomery potential and density. The present formulation may also provide a stepping stone to a model allowing time dependence and so incorporate a seasonally varying mixed-layer pulsing fluid into the thermocline.

Acknowledgments. We should like to thank P. P. Niiler for a very short but instructive encounter during Easter 1987 that led us to read his and P. S. Dubbelday's paper. We also acknowledge many productive discussions with R. Williams of Imperial College.

A. J. G. Nurser was supported in part by the Natural Environment Research Council and by the Ministry of Defence of the United Kingdom.

APPENDIX

The Thermodynamic Equation

The steady thermodynamic equation (7)

$$\frac{1}{\bar{\rho} f}\,\mathbf{k} \times \nabla p_s \cdot \nabla \rho_m = -\frac{\alpha_E \mathscr{H}_{\text{net}}}{h c_W}$$

is now transformed into a single equation in ρ_m. In order to do this we exploit the fact that $p_s \equiv p_s(D, f, \rho_m) \equiv p_s(\rho_m, x, y)$.

The surface pressure gradient is expressed in terms of the gradients of D and ρ_m. From (16), $p_s = p_s(D, \rho_m, f)$, and so

$$\nabla p_s = \left(\frac{\partial p_s}{\partial D}\right)\nabla D + \left(\frac{\partial p_s}{\partial f}\right)\nabla f + \left(\frac{\partial p_s}{\partial \rho_m}\right)\nabla \rho_m.$$

Now the Sverdrup constraint is used to eliminate ∇D. By (21), we have $P' = P'(\rho_m, D, f)$, so, taking the gradient,

$$\nabla P' = \left(\frac{\partial P'}{\partial D}\right)\nabla D + \left(\frac{\partial P'}{\partial f}\right)\nabla f + \left(\frac{\partial P'}{\partial \rho_m}\right)\nabla \rho_m.$$

Eliminating ∇D gives

$$\nabla p_s = A\nabla P' + B\nabla f + C\nabla \rho_m$$

where

$$A = \left(\frac{\partial p_s}{\partial D}\right) \Big/ \left(\frac{\partial P'}{\partial D}\right)$$

$$B = \frac{\partial p_s}{\partial f} - \left(\frac{\partial p_s}{\partial D}\right)\left(\frac{\partial P'}{\partial f}\right) \Big/ \left(\frac{\partial P'}{\partial D}\right)$$

and

$$C = \frac{\partial p_s}{\partial \rho_m} - \left(\frac{\partial p_s}{\partial D}\right)\left(\frac{\partial P'}{\partial \rho_m}\right) \Big/ \left(\frac{\partial P'}{\partial D}\right).$$

Therefore,

$$\mathbf{k} \times \nabla p_s \cdot \nabla \rho_m = (A\mathbf{k} \times \nabla P' + B\mathbf{k} \times \nabla f) \cdot \nabla \rho_m$$

since $\mathbf{k} \times \nabla \rho_m$ cannot advect ρ_m. Thus we arrive at (22)

$$\mathbf{u}_c \cdot \nabla \rho_m = -\frac{\alpha_E \mathscr{H}_{\text{net}}}{hc_W}$$

where the characteristic velocity $\mathbf{u}_c$ is

$$\mathbf{u}_c = (A\mathbf{k} \times \nabla P' + B\mathbf{k} \times \nabla f)/(\bar{\rho} f).$$

REFERENCES

Huang, R. X., 1988a: On boundary value problems of the ideal-fluid thermocline. *J. Phys. Oceanogr.*, **18,** 619–641.

——, 1988b: Ideal-fluid thermocline with weakly convective adjustment in a subpolar basin. *J. Phys. Oceanogr.*, **18,** 642–651.

——, 1989: On the three-dimensional structure of the wind-driven circulation in the North Atlantic. *Dyn. Atmos. Oceans,* **15,** 117–159.

Luyten, J. R., and H. Stommel, 1986a: A beta-control of buoyancy-driven geostrophic flows. *Tellus,* **38A,** 88–91.

——, and ——, 1986b: Gyres driven by combined wind and buoyancy flux. *J. Phys. Oceanogr.*, **16,** 1551–1560.

——, and ——, 1986c: Experiments with cross-gyre flow patterns on a beta-plane. *Deep-Sea Res.*, **33,** 963–972.

——, J. Pedlosky, and H. Stommel, 1983: The ventilated thermocline. *J. Phys. Oceanogr.*, **13,** 292–309.

Marshall, J. C., and A. J. G. Nurser, 1988: On the recirculation of the subtropical gyre. *Quart. J. Roy. Meteor. Soc.*, **114,** 1517–1534.

Needler, G., 1967: A model for the thermohaline circulation in an ocean of finite depth. *J. Mar. Res.*, **25,** 329–342.

Niiler, P. P., and P. S. Dubbelday, 1970: Circulation in a wind-swept and cooled ocean. *J. Mar. Res.*, **28**(2), 135–149.

Nurser, A. J. G., 1988: The distortion of a baroclinic Fofonoff gyre by wind forcing. *J. Phys. Oceanogr.*, **18,** 243–257.

——, and J. C. Marshall, 1991: On the relationship between subduction rates and diabatic forcing of the mixed layer. *J. Phys. Oceanogr.*, **21,** 1793–1802

Pedlosky, J., and W. R. Young, 1983: Ventilation, potential-vorticity homogenization and the structure of the ocean circulation. *J. Phys. Oceanogr.*, **13,** 2020–2037.

Rhines, P. B., and W. R. Young, 1982: A theory of the wind-driven circulation. I. Mid-ocean gyres. *J. Mar Res.*, **40**(Suppl.), 559–596.

Veronis, G., 1988: Circulation driven by winds and surface cooling. *J. Phys. Oceanogr.*, **18,** 1920–1932.

Williams, R. G., 1989: The influence of air–sea interaction on the ventilated thermocline *J. Phys. Oceanogr.*, **19,** 1255–1267.

——, 1991: The role of the mixed-layer in setting the potential vorticity of the ventilated thermocline. *J. Phys. Oceanogr.*, **21,** 1803–1814.

Woods, J. D., 1985: Physics of thermocline ventilation. *Coupled Atmosphere–Ocean Models,* J. C. J. Nihoul, Ed., Elsevier,